Available online at www.sciencedirect.com
ScienceDirect
Journal of Sound and Vibration 301 (2007) 678–689
JOURNAL OF SOUND AND VIBRATION
www.elsevier.com/locate/jsvi

Static analysis of a passive vibration isolator with quasi-zero-stiffness characteristic

A. Carrella, M.J. Brennan, T.P. Waters*

Institute of Sound and Vibration Research, University of Southampton, Southampton, Hampshire SO17 1BJ, UK

Received 7 April 2006; received in revised form 17 October 2006; accepted 18 October 2006
Available online 8 December 2006

Abstract

The frequency range over which a linear passive vibration isolator is effective, is often limited by the mount stiffness required to support a static load. This can be improved upon by employing nonlinear mounts incorporating negative stiffness elements configured in such a way that the dynamic stiffness is much less than the static stiffness. Such nonlinear mounts are used widely in practice, but rigorous analysis, and hence a clear understanding of their behaviour is not readily available in the literature. In this paper, a simple system comprising a vertical spring acting in parallel with two oblique springs is studied. It is shown that there is a unique relationship between the geometry and the stiffness of the springs that yields a system with zero dynamic stiffness at the static equilibrium position. The dynamic stiffness increases monotonically with displacement either side of the equilibrium position, and this is least severe when the oblique springs are inclined at an angle between approximately 48° and 57°. Finally, it is shown that the force–displacement characteristic of the system can be approximated by a cubic equation.

1. Introduction

Isolation of undesirable vibrations is a problem that affects many engineering structures. In the ideal case of a mass m supported by a linear stiffness k on a rigid foundation, isolation does not occur until a frequency of $\sqrt{2k/m}$. It is evident that a smaller stiffness results in a wider frequency range of isolation. However, a smaller stiffness results in a larger static displacement of the mass, and this trade-off between isolation and static displacement is well known [1,2]. To overcome this limitation nonlinear springs have been used to obtain a high static stiffness and hence a small static displacement, and a small dynamic stiffness, which results in a low natural frequency [3,4]. By careful choice of system parameters it is possible to achieve an isolator with zero dynamic stiffness, a so-called *quasi-zero-stiffness* (QZS) mechanism [5,6]. Applications of QZS mechanisms range from space research (e.g. to simulate zero gravity, [7]) to isolation of high-precision machinery [8]. Systems with quasi-zero-stiffness characteristic are of interest also in other fields, for example in geodynamics [9–11]. The precision of instruments such as *seismographs* or *gravimeters* requires very long periods of oscillation.

*Corresponding author.
E-mail address: tpw@isvr.soton.ac.uk (T.P. Waters).

0022-460X/$ - see front matter © 2006 Elsevier Ltd. All rights reserved.
doi:10.1016/j.jsv.2006.10.011

QZS mechanisms are generally achieved by combining a negative stiffness element with a positive stiffness element. A number of configurations have been proposed, many of which use nonlinearities such as spring orientation or buckling to create the negative stiffness effect [3,4]. Perhaps the simplest of these is shown in its unloaded condition in Fig. 1. When it is loaded with a suitably sized mass, the springs compress such that the oblique springs, k_o are in the horizontal position and the static load is taken by the vertical spring, k_v. This is the static equilibrium position, and it is the motion about this position that is of primary interest. When the system of springs is used in this way, the oblique springs act as a negative stiffness in the vertical direction counteracting the positive stiffness of the vertical spring. A typical force–deflection curve for the system in Fig. 1 is shown in Fig. 2, where the changing stiffness as a function of displacement can be seen. For the particular case shown in Fig. 2 the geometry and stiffness are chosen such that at the static equilibrium position, x_e, the dynamic stiffness is zero. The penalty for this, however, is that the system becomes stiffer than the vertical spring alone for large excursions from this position.

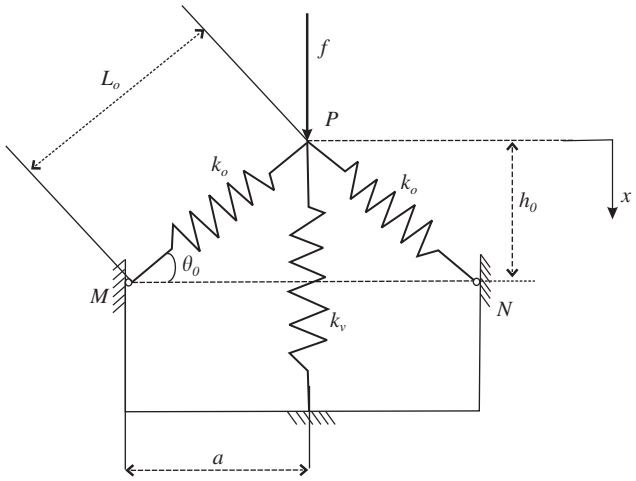

Fig. 1. Schematic representation of the simplest system which can exhibit quasi-zero stiffness.

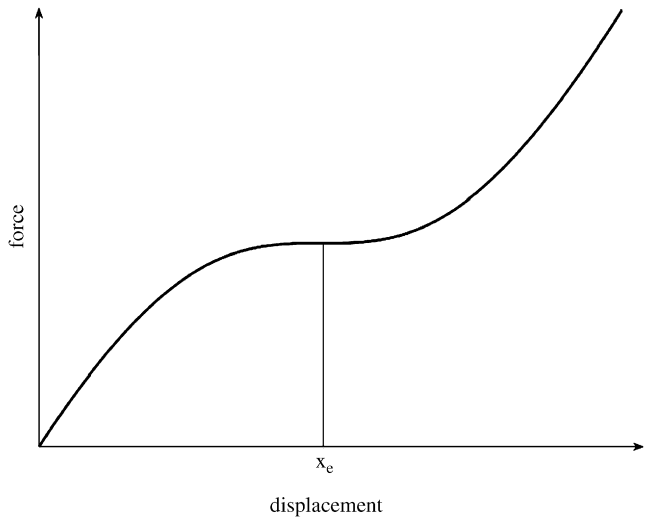

Fig. 2. Typical force–displacement characteristic of the isolator shown in Fig. 1.

In this paper, this trade-off between achieving a low dynamic stiffness for small excursions and acceptable stiffness for large excursions is investigated. An optimum relationship between the ratio of the oblique spring stiffness and the vertical spring stiffness is sought, as is an optimum angle for the oblique springs.

2. Force–displacement characteristic of a system with two oblique springs

It is instructive to examine first the behaviour of the oblique springs alone. Consider the system in Fig. 1, but with the vertical spring k_v removed. The two linear springs each of stiffness k_o hinged at points M and N, respectively, have initial length L_0. A force f is applied at point P which is a horizontal distance a from points M and N and initially at height h_0 above these points. The springs are initially at an angle θ_0 from the horizontal. The vertical component of the applied force is related to the spring stiffness k_o by

$$f = 2k_o(L_0 - L)\sin\theta, \tag{1}$$

where L is the length of the compressed spring, and $\sin\theta = (h_0 - x)/L$. Noting that $L_0 = \sqrt{h_0^2 + a^2}$ and $L = \sqrt{(h_0 - x)^2 + a^2}$, Eq. (1) can be written as

$$f = 2k_o(h_0 - x)\left(\frac{\sqrt{h_0^2 + a^2}}{\sqrt{(h_0 - x)^2 + a^2}} - 1\right), \tag{2}$$

which can be written in non-dimensional form as

$$\frac{f}{k_o L_0} = 2(\sqrt{1 - \gamma^2} - \hat{x})\left\{\left[\hat{x}^2 - 2\sqrt{1 - \gamma^2}\hat{x} + 1\right]^{-1/2} - 1\right\}, \tag{3}$$

where $\hat{x} = x/L_0$ and

$$\gamma = \frac{a}{L_0} = \cos\theta_0 \tag{4}$$

is a *geometrical parameter*. When $\gamma = 0$ the springs are initially vertical and when $\gamma = 1$ the springs, initially, lie horizontally. Fig. 3 shows the non-dimensional force plotted against the non-dimensional displacement for different values of γ.

It can be seen that the system has a highly nonlinear characteristic. The turning points of the curves represent zero stiffness but are unstable and the mechanism will "snap through" to a stable position if forced

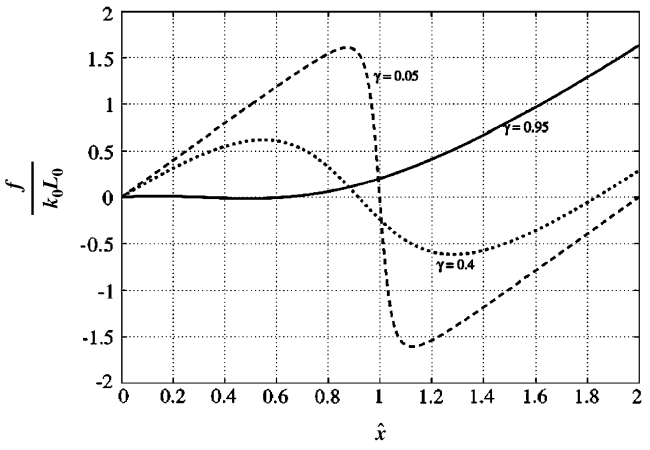

Fig. 3. Force–deflection characteristic of the system in Fig. 1. When $\gamma = 0$ the springs are vertical and when $\gamma = 1$ they are horizontal. The stiffness is negative between the maxima and the minima.

into this region. The maximum non-dimensional force that the system can accept before it snaps through is given by

$$\frac{f_{\max}}{k_o L_0} = 2\left[1 - \left(1 - \sqrt{1-\gamma^2}\right)^{1/3}\right]^{3/2}, \tag{5}$$

which occurs at

$$\hat{x}_{\max} = \sqrt{1-\gamma^2} - \gamma\sqrt{\gamma^{-2/3} - 1}. \tag{6}$$

The non-dimensional stiffness, K/k_o, of this system can be calculated by differentiating the force with respect to the displacement to give

$$\frac{K}{k_o} = 2\left[1 - \frac{\gamma^2}{\left(\hat{x}^2 - 2\sqrt{1-\gamma^2}\hat{x} + 1\right)^{3/2}}\right]. \tag{7}$$

The stiffness is a minimum at the equilibrium position, $\hat{x}_e = \sqrt{1-\gamma^2}$, and is given by

$$\frac{K}{k_o} = 2\left(1 - \frac{1}{\gamma}\right), \tag{8}$$

which becomes increasingly negative as the angle of inclination of the springs is increased.

The system can be modified to exhibit QZS at a point of stability by adding a vertical spring of equal and opposite (positive) stiffness, and such a system is the focus of the following section.

3. A QZS mechanism

For the system in Fig. 1, the vertical spring k_v is in parallel with the vertical components of the oblique springs. Choosing now to non-dimensionalise force f by $k_v L_0$, the resulting non-dimensional spring force $\hat{f}$ is given by

$$\hat{f} = \hat{x} + 2\alpha(\sqrt{1-\gamma^2} - \hat{x})\left\{\left[\hat{x}^2 - 2\sqrt{1-\gamma^2}\hat{x} + 1\right]^{-1/2} - 1\right\}, \tag{9}$$

where $\alpha = k_o/k_v$ is the ratio of the spring stiffnesses. For large α Eq. (9) tends to Eq. (3).

The non-dimensional stiffness of the system can be found by differentiating Eq. (9) with respect to the displacement to give

$$\hat{K} = 1 + 2\alpha\left[1 - \frac{\gamma^2}{\left(\hat{x}^2 - 2\sqrt{1-\gamma^2}\hat{x} + 1\right)^{3/2}}\right]. \tag{10}$$

The non-dimensional force as a function of the non-dimensional displacement is plotted in Fig. 4 for several values of γ and when $\alpha = 1$. For large initial angles (such as $\gamma = 0.05$ and 0.4 in Fig. 4) the inclined springs dominate the behaviour resulting in a region of negative stiffness. For small initial angles of inclination, such as $\gamma = 0.95$, the vertical spring dominates such that the combined stiffness of the mechanism is always positive and only weakly nonlinear. At a unique intermediate angle of inclination, represented by γ_{QZS}, there is a stationary point of inflexion, which corresponds to a stable equilibrium position with zero stiffness. This occurs at the equilibrium position $\hat{x}_e = \sqrt{1-\gamma^2}$ at which the (maximum) negative stiffness from the inclined springs is exactly balanced by the positive stiffness of the vertical spring. This is seen more clearly in Fig. 5 in which the non-dimensional stiffness is plotted as a function of the non-dimensional displacement for the same set of parameter values.

There is a unique relationship between the geometrical parameter $\gamma = a/L_0$ and the spring coefficient ratio $\alpha = k_o/k_v$ that yields the desired stable QZS characteristic. If Eq. (10) is evaluated at the static equilibrium

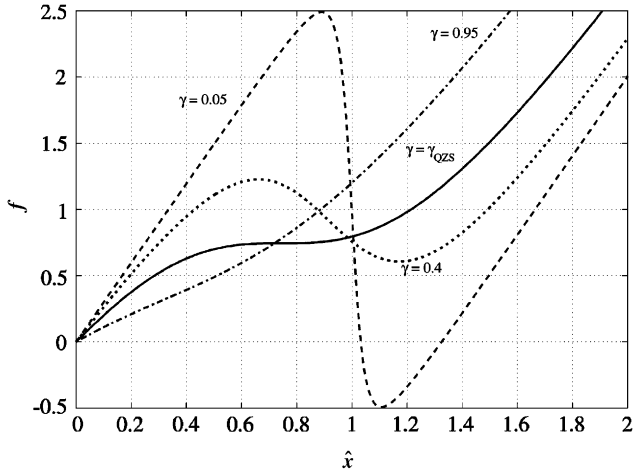

Fig. 4. Force–displacement characteristic of the three spring system when $\alpha = 1$: the solid line is the QZS system.

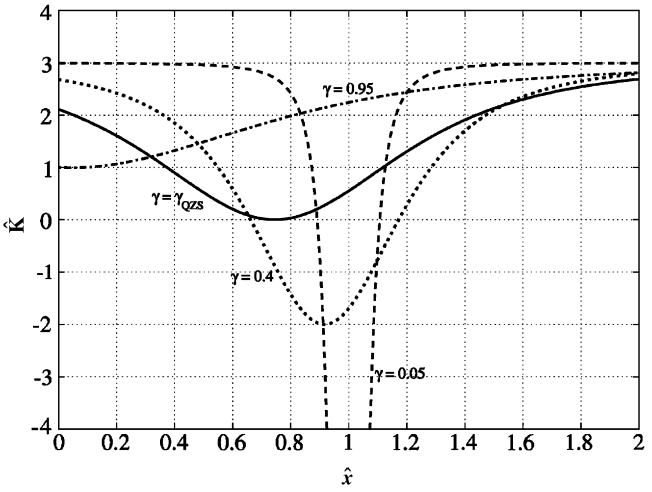

Fig. 5. Non-dimensional stiffness of a QZS mechanism when $\alpha = 1$: the solid line is representative of a stable system (always positive stiffness) with zero stiffness at the static equilibrium position. The stiffness is very small (quasi-zero) for a small deviation from this position.

position $\hat{x}_e = \sqrt{1-\gamma^2}$ and set to zero, then the value γ_{QZS} that gives quasi-zero-stiffness is

$$\gamma_{\mathrm{QZS}} = \frac{2\alpha}{2\alpha + 1} \tag{11a}$$

for a given value of α. Equivalently, the value of α that ensures QZS behaviour for a given γ is

$$\alpha_{\mathrm{QZS}} = \frac{\gamma}{2(1-\gamma)}. \tag{11b}$$

Hereafter, the subscript QZS on either α or γ is used to denote that the other parameter is not independent, but has been chosen in accordance with Eq. (11) so as to achieve stable QZS.

The combinations of stiffness ratio α and geometrical parameter γ that give rise to stable QZS are shown in graphical form in Fig. 6. For small initial angles ($\gamma \approx 1$) the inclined springs need to be orders of magnitude larger than the vertical spring. When the initial angle of inclination is a moderate 37°–66°, say, ($0.4 < \gamma < 0.8$)

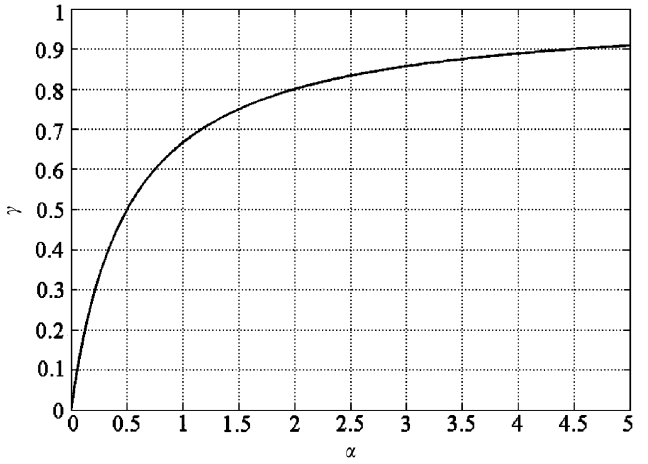

Fig. 6. Combinations of geometrical parameter γ and stiffness ratio α that yield QZS.

then vertical and inclined springs of similar stiffnesses can be employed, although this will result in larger static deformations of the springs.

4. Optimisation of the QZS mechanism

Although Eqs. (11a), (11b) relate the geometrical and stiffness parameters to give a QZS system, there is an infinite number of possible combinations of these parameters. However, the range of displacements over which the stiffness is smaller than the vertical spring alone, for example, is very much dependent upon the geometrical parameter. This relationship is explored further in this section.

By enforcing the QZS condition on α and γ in Eq. (11), the non-dimensional stiffness given by Eq. (10) can be written as a function of just the geometrical parameter as

$$\hat{K}_{\mathrm{QZS}} = 1 + \frac{\gamma_{\mathrm{QZS}}}{(1-\gamma_{\mathrm{QZS}})}\left[1 - \frac{\gamma_{\mathrm{QZS}}^2}{\left(\hat{x}^2 - 2\sqrt{1-\gamma_{\mathrm{QZS}}^2}\hat{x} + 1\right)^{3/2}}\right]. \tag{12}$$

This is plotted in Fig. 7 for several values of γ_{QZS}. It can be seen from the figure that the stiffness is zero at the static equilibrium position, $\hat{x}_e = \sqrt{1-\gamma_{\mathrm{QZS}}^2}$, and the displacement range over which there is a small stiffness depends on γ_{QZS}.

Of interest is the range of displacements about the equilibrium position for which the stiffness is less than a prescribed stiffness $\hat{K}_o$, say. (Note that a value of $\hat{K}_o = 1$ means that the stiffness of the system is equal to that of the vertical spring.) The displacement at which the stiffness is equal to the threshold value is found by setting $\hat{K}_{\mathrm{QZS}} = \hat{K}_o$ in Eq. (12) and solving for $\hat{x}$, which yields

$$\hat{x}|_{\hat{K}=\hat{K}_o} = \hat{x}_e \pm \hat{d}, \tag{13}$$

where $\hat{x}_e$ is the static equilibrium position and $\hat{d}$ is the excursion, normalised by L_0, from this position when $\hat{K} = \hat{K}_o$, and is given by

$$\hat{d} = \gamma_{\mathrm{QZS}}\sqrt{\left[\frac{1}{1-\hat{K}_o(1-\gamma_{\mathrm{QZS}})}\right]^{2/3} - 1}. \tag{14}$$

This is plotted in Fig. 8 as a function of γ_{QZS} for various values of $\hat{K}_o$. It can be seen that the value of γ_{QZS} for which $\hat{d}$ is a maximum, changes depending on the value of $\hat{K}_o$. It is not possible to determine a closed-form

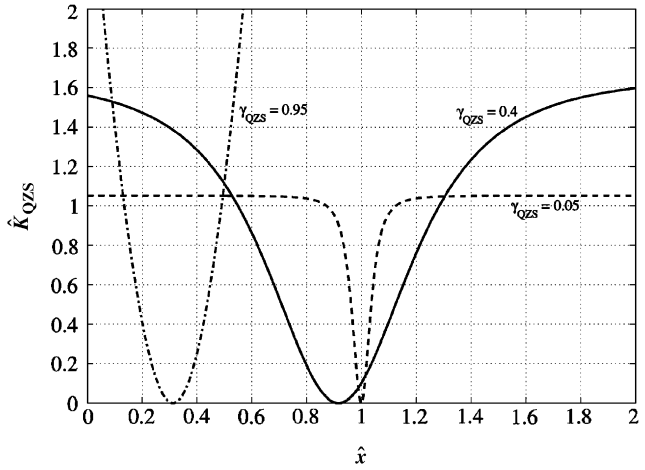

Fig. 7. Non-dimensional stiffness for different combinations of geometrical and stiffness parameters that yield QZS.

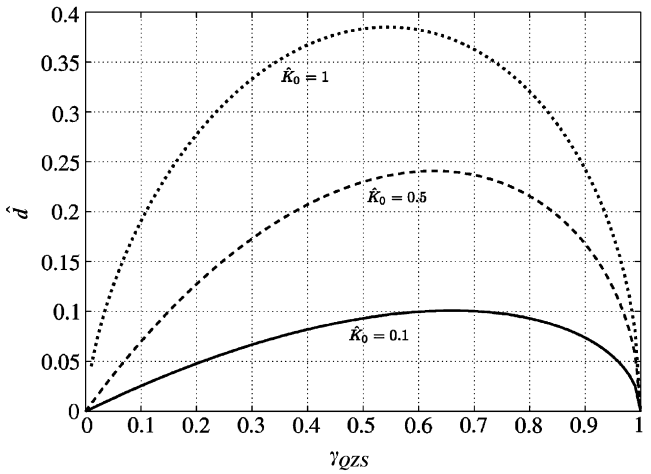

Fig. 8. Non-dimensional displacement from the static equilibrium position as a function of γ_{QZS}.

solution for this from Eq. (14), but it can be evaluated when $\hat{K}_o \ll 1$ and when $\hat{K}_o = 1$. For the case when $\hat{K}_o \ll 1$ Eq. (14) can be approximated by

$$\hat{d} \approx \gamma_{QZS}\sqrt{\frac{2}{3}\hat{K}_o(1-\gamma_{QZS})}, \tag{15}$$

which when differentiated with respect to γ_{QZS}, and set to zero gives the optimal geometrical parameter

$$\gamma_{opt} = \frac{2}{3}, \quad \hat{K}_o \ll 1. \tag{16}$$

If this is substituted into Eq. (11b) the optimum value of the stiffness ratio is $\alpha_{opt} = 1$, which means that all the springs have the same stiffness. If $\hat{K}_o$ is set to unity in Eq. (14) and the same procedure followed, the optimum geometrical parameter is found to be

$$\gamma_{opt} = \left(\frac{2}{3}\right)^{3/2}, \quad \hat{K}_o = 1. \tag{17}$$

An approximate general expression that relates γ and $\hat{K}_o$ for values of $0 \leqslant \hat{K}_o \leqslant 1$ can be determined by assuming a relationship of the form

$$\gamma_{\text{opt}} \approx \left(\frac{2}{3}\right)^{c_1\hat{K}_o + c_2}. \tag{18}$$

The constants c_1 and c_2 can be found by using Eqs. (16) and (17) for $\hat{K}_o = 0$ and 1, respectively, to give

$$\gamma_{\text{opt}} \approx \left(\frac{2}{3}\right)^{(\hat{K}_o/2)+1}. \tag{19}$$

This shows that there is only a weak relationship between the optimum geometry and the prescribed maximum stiffness of the system in which the angle for the oblique springs ranges from about 48° to 57°. The corresponding optimum stiffness ratio α_{opt} ranges from 1 to 0.6.

By substituting Eq. (19) into Eq. (14) an expression can be found that gives the maximum excursion from the static equilibrium position as a function of the maximum stiffness of the system during this excursion. It is given by

$$\hat{d} = \left(\frac{2}{3}\right)^{(\hat{K}_o/2)+1} \sqrt{\frac{1}{\left\{1 - \hat{K}_o\left[1 - \left(\frac{2}{3}\right)^{(\hat{K}_o/2)+1}\right]\right\}^{2/3}} - 1}. \tag{20}$$

Fig. 9 shows the largest excursion from the static equilibrium position that can be achieved without the system having stiffness larger than $\hat{K}_o$. The solid line is the solution calculated using Eq. (14), where the optimum value of γ_{QZS} for a given $\hat{K}_o$ is determined numerically. The dotted line is calculated using Eq. (20). Note that there is very little difference between the two solutions.

If the allowable increase in stiffness due to excursions about the equilibrium position is small, i.e. $\hat{K}_o \ll 1$, then Eq. (20) can be expanded to give the approximate relationship

$$\hat{d} \approx \frac{2}{9}\sqrt{2\hat{K}_o}, \quad \hat{K}_o \ll 1. \tag{21}$$

The analysis presented so far is based on the assumption that γ_{QZS} and α_{QZS} are related by Eq. (11). However, it is possible that, due to manufacturing tolerances Eq. (11) may not hold exactly. The question is whether the behaviour of the system is very sensitive to a change in the stiffness ratio. To investigate

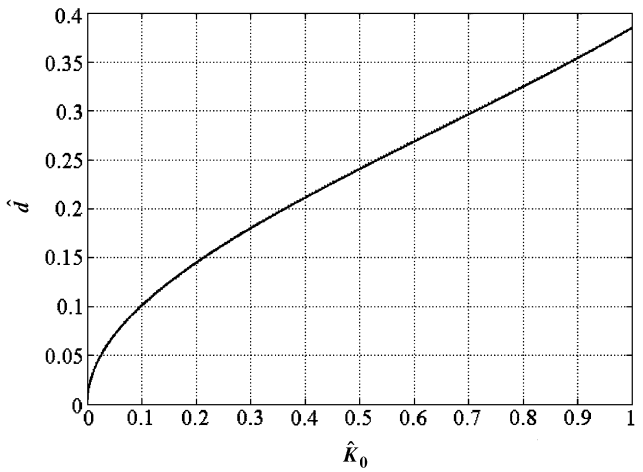

Fig. 9. Numerical and analytical representation of the maximum excursion from the static equilibrium position, $\hat{d}$, over which the system has a stiffness smaller than $\hat{K}_0$. (— numerical; -- equation (20)).

this let there be a fractional deviation ε from α_{QZS} such that $\alpha = \alpha_{QZS}(1 \pm \varepsilon)$. Substituting this into Eq. (10) gives

$$\hat{K} = \hat{K}_{QZS} \pm 2\varepsilon\alpha_{QZS}\left[1 - \frac{\gamma_{QZS}^2}{\left(\hat{x}^2 - 2\sqrt{1-\gamma_{QZS}^2}\hat{x} + 1\right)^{3/2}}\right], \tag{22}$$

where $\hat{K}_{QZS}$ is the stiffness when $\alpha = \alpha_{QZS}$ and $\gamma = \gamma_{QZS}$. Since excursions about the static equilibrium position are of interest the stiffness is evaluated at this position, where $\hat{K}_{QZS} = 0$. Substituting $\hat{x} = \hat{x}_e = \sqrt{1-\gamma^2}$ into Eq. (22) results in

$$\hat{K}\big|_{\hat{x}=\hat{x}_e} = -(\pm\varepsilon). \tag{23}$$

This means that the non-dimensional stiffness of the system at the static equilibrium position is of equal magnitude but opposite sign to the fractional change in the stiffness ratio at the static equilibrium position. Thus, for example, if the spring ratio is 1% smaller than α_{QZS} then the dimensional stiffness of the system at the static equilibrium position, which should be zero in optimal conditions, will be $0.01k_v$.

Although there are benefits to incorporating springs configured to act as a negative stiffness, there are also some disadvantages. As shown in Fig. 3, the oblique springs only act as a negative stiffness over a certain displacement range. Outside this range they act as a positive stiffness, adding to the stiffness of the vertical spring. This can be seen in Fig. 5. The peak positive stiffness can be obtained by setting $x \gg h_0$ such that $\hat{x} \gg 1$ and Eq. (12) becomes

$$\hat{K}\big|_{x \gg h_0} = \frac{1}{1-\gamma_{QZS}}. \tag{24}$$

The optimal value for γ_{QZS} lies between 2/3 and $(2/3)^{3/2}$ depending on the stringency with which low stiffness is required. Thus, the cost of having a QZS mechanism is that for large excursions from the static equilibrium position the stiffness can increase to between about two and three times that of the vertical spring.

5. Approximation to the stiffness of the QZS isolator

The relationship between force and displacement given in Eq. (9) and shown graphically in Fig. 2 is similar to that of a cubic function. It would considerably simplify subsequent dynamic analysis of the QZS system if its stiffness could be described by a polynomial. A simplified cubic expression of the force is therefore sought and the error in the approximation quantified.

Using a Taylor series expansion, the force can be expressed as a power series of order N [12]

$$f(y) = f(y_0) + \sum_{n=1}^{N} \frac{f^n(y_0)}{n!}(y - y_0)^n, \tag{25}$$

where y_0 is the point at which the function is expanded and f^n denotes the nth derivative of f. Since the displacement of the system about the static equilibrium position is of interest, the power series for the force is expanded about this point. By expanding Eq. (9) using Eq. (25) and substituting for $\hat{y} = \hat{x} - \sqrt{1-\gamma^2}$ an approximate expression for the force is found to be

$$\hat{f}(\hat{y}) \approx \frac{\alpha}{\gamma^3}\hat{y}^3 + \left[1 - 2\alpha\frac{(1-\gamma)}{\gamma}\right]\hat{y} + \sqrt{1-\gamma^2}, \tag{26}$$

which consists of a cubic term, a linear term and a constant term. An approximate expression for the stiffness can be obtained by differentiating Eq. (26) to give

$$\hat{K} \approx 3\frac{\alpha}{\gamma^3}\hat{y}^2 + \left[1 - 2\alpha\frac{(1-\gamma)}{\gamma}\right]. \tag{27}$$

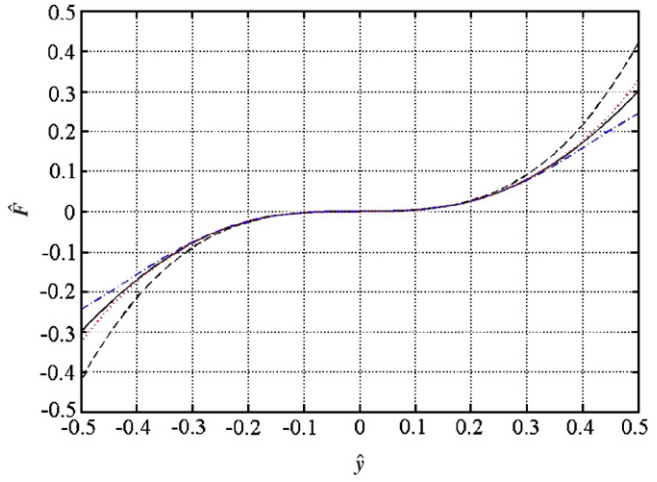

Fig. 10. Force–displacement characteristic of the QZS mechanism when $\gamma = 2/3$ and $\alpha = 1$. (— exact expression; - - - third-order expansion; - · - fifth-order expansion; .... seventh-order expansion).

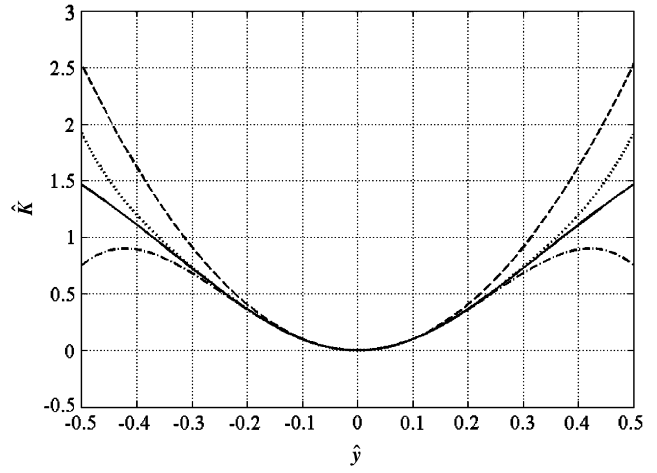

Fig. 11. Stiffness of the QZS mechanism as a function of deflection when $\gamma = 2/3$ and $\alpha = 1$. (— exact expression; - - - third-order expansion; - · - fifth-order expansion; .... seventh-order expansion).

If γ and α are chosen according to Eq. (11), the linear term in Eq. (26) disappears. Moreover, if the force is transformed by $\hat{F} = \hat{f} - \sqrt{1-\gamma_{\mathrm{QZS}}^2}$ to remove the constant term, then Eq. (26) can be written as

$$\hat{F}(\hat{y}) = \frac{1}{2\gamma_{\mathrm{QZS}}^2(1-\gamma_{\mathrm{QZS}})}\,\hat{y}^3, \tag{28}$$

which is plotted in Fig. 10. Also shown in the same figure are the curves corresponding to the approximation to the force if the fifth- and seventh-order terms in the series are included. Differentiating Eq. (28) gives the approximate stiffness of the QZS system to be

$$\hat{K}_{\mathrm{QZS}} \approx \frac{3}{2}\frac{1}{\gamma_{\mathrm{QZS}}^2(1-\gamma_{\mathrm{QZS}})}\,\hat{y}^2, \tag{29}$$

which is shown in Fig. 11, again compared with higher-order expansions.

The error between the approximate stiffness and the actual stiffness increases as the displacement from the static equilibrium position increases. This can be quantified at the maximum excursion when the stiffness

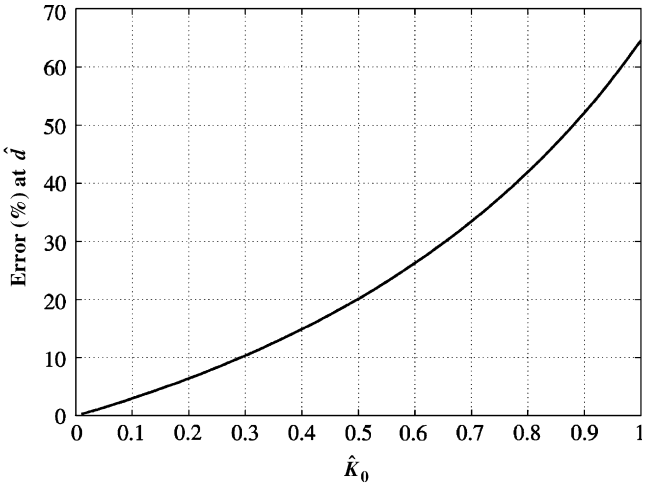

Fig. 12. Error in the approximation for the stiffness evaluated at the maximum excursion from the static equilibrium position such that the stiffness is smaller than $\hat{K}_0$.

equals $\hat{K}_o$ by the following:

$$\text{error}(\%) = \left| 1 - \frac{\hat{K}_{\text{approximate}}}{\hat{K}_{\text{actual}}} \right| \times 100, \tag{30}$$

where $\hat{K}_{\text{approximate}}$ is given by Eq. (29) and $\hat{K}_{\text{exact}}$ is given by Eq. (12), both evaluated at the maximum excursion for the corresponding $\hat{K}_o$. The percentage error is plotted in Fig. 12. It can be seen that the error is relatively small if the threshold stiffness $\hat{K}_o$ and hence the excursion from the static equilibrium position are small, but is significant as the threshold stiffness becomes comparable to that of the vertical spring ($\hat{K}_o \sim 1$).

6. Conclusions

The static characteristics of a quasi-zero stiffness mechanism have been investigated. The main feature of such a mechanism is the use of a negative stiffness element to achieve a low stiffness without having a large static deflection. A simple system consisting of three springs has been studied, and the optimum relationship between the geometry and the relative stiffnesses of the springs has been investigated. It has been found that to achieve a large excursion from the static equilibrium position such that the stiffness of the system does not exceed a prescribed value, there is an optimum geometry and a corresponding optimum relationship between the stiffnesses. It has also been found that for the spring configuration studied the oblique springs have to be inclined at an angle between approximately 48° and 57°. An approximate polynomial expression for the stiffness of the system has also been determined and the errors in this expression compared to the exact expression have been quantified.

References

[1] J.P. Den Hartog, *Mechanical Vibrations*, McGraw-Hill, New York, 1956.
[2] C.M. Harris, A.G. Piersol, *Shock and Vibration Handbook*, fifth ed., McGraw-Hill, New York, 2002.
[3] E.I. Rivin, *Passive Vibration Isolation*, ASME Press, New York, 2001.
[4] P. Alabuzhev, A. Gritchin, L. Kim, G. Migirenko, V. Chon, P. Stepanov, *Vibration Protecting and Measuring Systems with Quasi-Zero Stiffness*, Hemisphere Publishing, New York, 1989.
[5] D.L. Platus, Negative-stiffness-mechanism vibration isolation systems, *SPIE—Vibration Control in Microelectronics, Optics and Metrology* 1619 (1991) 44–54.
[6] J. Zhang, D. Li, S. Dong, An ultra-low frequency parallel connection nonlinear isolator for precision instruments, *Key Engineering Materials* 257–258 (2004) 231–236.

[7] K. Denoyer, C. Johnson, Recent achievements in vibration isolation systems for space launch and on-orbit applications, *52nd International Astronautical Congress*, Toulouse, France, 2001.
[8] J. Dankowski, State of the art vibration isolation of large coordinate measuring machine with an adverse environment, *Second Euspen International Conference*, Turin, Italy, 2001.
[9] P. Lorrain, Low natural frequency vibration isolator or seismograph, *Review of Scientific Instruments* 45 (1974) 198–202.
[10] L. Lacoste, Lacoste and Romberg straight-line gravity meter, *Geophysics* 48 (1983) 606–610.
[11] J. Winterflood, High Performance Vibration Isolation for Gravitational Wave Detection, PhD Thesis, University of Western Australia—Department of Physics, 2001.
[12] E.T. Whittaker, G.N. Watson, *A Course of Modern Analysis*, fourth ed., Cambridge Mathematical Library, 1990.